

## **General Disclaimer**

### **One or more of the Following Statements may affect this Document**

- This document has been reproduced from the best copy furnished by the organizational source. It is being released in the interest of making available as much information as possible.
- This document may contain data, which exceeds the sheet parameters. It was furnished in this condition by the organizational source and is the best copy available.
- This document may contain tone-on-tone or color graphs, charts and/or pictures, which have been reproduced in black and white.
- This document is paginated as submitted by the original source.
- Portions of this document are not fully legible due to the historical nature of some of the material. However, it is the best reproduction available from the original submission.

X-620-68-414

PREPRINT

NASA TM X- 63391

# MICROWAVE OBSERVATIONS OF SEA STATE FROM AIRCRAFT

W. NORDBERG  
JACK CONAWAY  
P. THADDEUS

NOVEMBER 1968



GODDARD SPACE FLIGHT CENTER

GREENBELT, MARYLAND

N 69-11537

FACILITY FORM 602

(ACCESSION NUMBER)

24  
(PAGES)

(THRU)

(CODE)

(NASA CR OR TMX OR AD NUMBER)

(CATEGORY)



MICROWAVE OBSERVATIONS OF  
SEA STATE FROM AIRCRAFT

W. Nordberg

Jack Conaway

P. Thaddeus

November 1968

(Submitted for Publication to Quart. Jour. Roy. Met. Soc.)

GODDARD SPACE FLIGHT CENTER

Greenbelt, Maryland

MICROWAVE OBSERVATIONS OF  
SEA STATE FROM AIRCRAFT

W. Nordberg

Jack Conaway

P. Thaddeus

November 1968

GODDARD SPACE FLIGHT CENTER

Greenbelt, Maryland

## CONTENTS

	<u>Page</u>
INTRODUCTION. . . . .	1
NATURE OF OBSERVED RADIATION. . . . .	2
DISCUSSION OF MEASUREMENTS. . . . .	5
CONCLUSIONS. . . . .	11
REFERENCES. . . . .	13

# MICROWAVE OBSERVATIONS OF SEA STATE FROM AIRCRAFT

W. Nordberg, Jack Conaway, and P. Thaddeus

NASA, Goddard Space Flight Center

Greenbelt, Maryland

## INTRODUCTION

Following a suggestion by Buettner (1963), we have measured the thermal radiation emitted by the Earth at a wavelength of 1.55 cm from altitudes up to 12 km with a Convair-990 jet aircraft. The main purpose of these measurements was to relate observed variations in radiant emittance to variations in the amounts of liquid water contained in clouds, and to determine the feasibility of performing such measurements from satellites. An electrically scanning radiometer developed especially for this purpose by the Aerojet General Corporation of El Monte, California was installed on the aircraft. It consisted of: a phased array antenna which accepts radiation in a beam about  $2.8^\circ$  wide (the beam was electrically scanned perpendicular to the aircraft's flight direction, along a line extending  $\pm 50^\circ$  from nadir); a receiver measuring the detected radiation with an accuracy corresponding to about  $\pm 1^\circ\text{C}$  of equivalent Brightness Temperature; and associated calibration and recording equipment. The radiometer, and results from about 100 hours of aircraft flights over a wide

variety of atmospheric and surface conditions are described by Oister (1967) and by Nordberg, et al. (1968), respectively. Here, we wish to report only on measurements of microwave radiances observed over water of varying surface conditions.

Theoretically, the radiation emitted by a water surface at 1.55 cm is expected to depend on the surface roughness at nadir angles greater than about 30° (Stogryn, 1967). We shall examine this dependence on the basis of our measurements and consider possible applications of passive microwave measurements from satellites to worldwide mapping of sea state. Such mapping would be of interest to meteorologists and oceanographers who wish to explore the transfer of energy between the ocean surface and the atmosphere on a global scale. It might also be of practical value to those interested in ocean navigation.

#### NATURE OF OBSERVED RADIATION

The spectral intensity  $I(\theta)$  of the radiation emitted at 1.55 cm in the direction of a nadir angle  $\theta$ , as viewed from the aircraft, is proportional to the absolute temperature  $T_w$  and the emissivity  $\epsilon$  of the surface:

$$I(\theta) \sim \epsilon(\theta) T_w \quad (1)$$

The product  $\epsilon T_w$  is commonly referred to as "brightness temperature,"  $T_B$ .

All our measurements are expressed in terms of that product and the radiometer is calibrated with reference to a radiation source of known brightness temperature.

Our measurements of  $T_B$  were made from altitudes ranging from about 20 m to about 12 km above the surface. At this wavelength, the absorption and re-emission of radiation by the atmosphere, due to the presence of water vapor, must be considered. The brightness temperature measured by the aircraft at the height can then be expressed as:

$$T_B(\theta, h) = \left( \epsilon(\theta) T_w + r(\theta) T_s \right) \tau(h) + \int_0^h T_A(h) \frac{\partial \tau}{\partial h} dh \quad (2)$$

Where  $T_s$  is the brightness temperature of the sky integrated over the entire hemisphere at the surface,  $T_A$  is the temperature of the atmosphere,  $r$  is the reflectivity of the sea surface and  $\tau$  is the transmissivity of the atmosphere.  $\tau$  can be expressed as:

$$\tau = \exp\left(-\sec \theta \int_0^h k \rho dh\right) \quad (3)$$

where  $\rho$  is the density of the absorbing gases,  $k$  is the absorption coefficient for these gases. At this wavelength, water vapor is the primary absorber. Eq. (2) holds for a cloudless atmosphere in which our measurements were made.  $T_B$ ,  $\epsilon$  and  $r$  depend on the polarization of the measured radiation. Since we measured only horizontally polarized radiation (electrical vector perpendicular to the scan direction and parallel to the earth's surface for level aircraft altitudes), we define Eq. (2) as written for horizontal polarization.

$\epsilon$  and  $r$  depend on the roughness of the water surface such that  $\epsilon$  increases and  $r$  decreases with increasing roughness. Since  $T_w \approx 300^\circ\text{K}$  and  $T_a < 70^\circ\text{K}$ ,  $T_B$  will increase with roughness. The exact nature of the relationship between surface roughness and emissivity is, as yet, poorly understood, as different scales of roughness, ranging from foam and spray to heavy swells, will produce qualitatively and quantitatively different effects on the emissivity. Taking into account the observation by Cox and Munk, that the slopes of ocean waves follow a nearly Gaussian distribution, Stogryn (1967) computed the dependence of  $\epsilon$  and  $r$  on the state of the sea surface. However, Stogryn's analysis did not include the effect of very small scale roughness such as bubbles, foam and spray.

On the basis of these computed functions for  $\epsilon$  and  $r$ , Stogryn integrated Eq. (2) for conditions ( $T_w = 290^\circ\text{K}$ ,  $T_a$  and  $k\rho$  for a cloudless Standard Atmosphere, and 1.55 cm wavelength) very similar to those under which we made our measurements. Therefore, we find it convenient to discuss our measurements in comparison with the results of Stogryn's analysis (Figure 1).

Aside from roughness, emissivity of water depends on salinity and temperature. The effect of salinity is negligible compared to roughness and, near 1.55 cm, a  $30^\circ\text{C}$  change in  $T_w$  will produce only a  $2^\circ\text{C}$  change in  $T_B$ . This is because an increase in the water surface temperature decreases the emissivity and thus, according to the proportionality (1),  $T_B$  is nearly independent of the water temperature. Furthermore, the distance range over which we observed variations

of  $T_B$  with water surface roughness was less than 30 km. Brightness temperature changes due to surface temperature variations observed within that range were always much smaller than those caused by the roughness variations. Variations in  $T_A$ ,  $T_S$ , and  $\tau$  were negligible within the range of our aircraft measurements shown here.

We recognize, however, that for global mapping of sea state from spacecraft, variations in  $T_s$  and  $\tau$  would be so large at this wavelength that they might produce variations in  $T_B$  comparable to those produced by sea surface roughness. For example, at 1.55 cm,  $\tau \approx 0.95$  for a typical, clear, mid-latitude atmosphere; but, in a moist atmosphere and in the presence of thick clouds,  $\tau$  may be as low as 0.5. In such cases, the unknown variation of cloudiness would completely mask the effect of sea surface roughness. At wavelengths longer than 3 cm, this effect would be greatly diminished and  $\tau$  would be very nearly 1, except for very thick clouds and for rainclouds. Spacecraft observations would, therefore, be made at these longer wavelengths. It is assumed that the effect of roughness on emissivity shown here is similar at the longer wavelengths. We hope to demonstrate this in future experiments.

## DISCUSSION OF MEASUREMENTS

Two cases are particularly prominent in our observations:

(1) A series of passes on 7 June 1968 over the Salton Sea (California) at heights ranging from 60 to 11,100 meters above the Sea surface, when the northwestern half of the sea was very smooth and calm, and the southeastern half was

driven by about 15 m/sec surface winds from a local disturbance. The demarkation between these surface conditions was extremely abrupt. We also made several passes over the Salton Sea two days earlier, however, abrupt roughness changes were not apparent then, as the sea was generally smooth.

(2) Two passes on 20 June 1968 over the Pacific Ocean off the coast of northern California at a height of about 10,000 m, when the ocean surface roughness changed abruptly from moderate (no white caps) to rough (frequent white caps) at a distance of about 20 km off shore (Figure 1).

A third case over the Eastern Shore of Maryland in May 1967 provided a similar difference between the rough Atlantic waters and a calm protected lagoon west of Assateague Island. In that case, aircraft maneuvers prevented us from obtaining as definite microwave measurements as in cases (1) and (2), but all indications are consistent with the conclusions presented here. All observations were made in cloudless skies.

Measurements of  $T_B$  over the Salton Sea are compared to Stogryn's (1967) analysis in Figure 2. The observations show a considerably greater difference of brightness temperatures between smooth and rough seas than indicated by theory. The measured differences are approximately the same ( $20^\circ\text{C}$ ) at all nadir angles. In contrast, the theoretical analysis calls for a difference of about  $15^\circ\text{C}$  at  $\theta = 40^\circ$ , and a steady decrease of this difference with decreasing nadir angle. At nadir, there should be practically no difference.

Over the smooth sea there is general agreement between the observations and theory, although the measured brightness temperatures are slightly lower than the computed ones: Stogryn's calculations yield a value of  $T_B = 137^\circ\text{K}$  at nadir for  $h = 1,000$  m, while our measurements show about  $133^\circ\text{K}$  at 1,500 m. At 40 degrees from nadir, the theoretical and observed values at these altitudes of  $T_B$  are  $123^\circ$  and  $121^\circ\text{K}$  respectively. At intermediate nadir angles, the observed values are about  $5^\circ\text{C}$  lower than those predicted by theory.

The surface windspeed over the rough water was about 15 m/sec; over the smooth water it was less than 3 m/sec. Windspeeds were obtained from aircraft drift measurements and from visual wave height estimates. Strong spray and very frequent white caps were visually observed over the rough, southeastern part of the sea, while the northwestern half of the Salton Sea displayed no white caps and presented a smooth, slightly rippled appearance. A sharp sun image could be seen in the water of this half of the sea. These visual observations were documented by photographs similar to Figure 1 taken continuously during all aircraft passes. In addition, we measured concurrently the equivalent black-body temperatures for the sea surface ( $T_{IR}$ ) with a Medium Resolution Infrared (MRIR) radiometer in the  $10.5\text{--}11.5\mu$  spectral range. This radiometer also measured the reflectance ( $R$ ) of solar radiation expressed in fractions of reflected radiation compared to incident radiation (Figure 3).

The large and almost constant brightness temperature difference between rough and smooth Sea for all nadir angles between 0 and 50 degrees was observed

at all heights between 500 m and 11,100 m. The rough sea presented a "limb darkening" effect (decrease of brightness temperature with nadir angle) equal to that of the smooth sea at all altitudes.

Figure 3 shows the recorded brightness temperatures at nadir as the aircraft passed along the northwest-southeast axis of the Salton Sea at four altitude levels. On each pass, the abrupt change in brightness temperature coincides with the demarkation line between the smooth and rough sea. The reflectance of solar radiation measured with the MRIR radiometer also shows an abrupt increase from the smooth to the rough sea, because of the greater reflectivity of foam, spray and white caps.  $T_B$  measurements, given on a time scale in Figure 3, may be related to distance from this demarkation line using the aircraft speed. At the low altitudes, the speed was about 9 km per minute and at the higher altitudes it was about 14 km per minute. Passes were made at seven height levels. For simplicity's sake, only four levels are shown in Figure 3. The water surface temperatures were 294°K for the rough Sea and 300°K for the smooth Sea. This is reasonable since one expects colder temperatures for the disturbed water. It is interesting to note that the 6°C difference in water temperature between the rough and smooth seas should have made the brightness temperatures slightly colder over the rough Sea. Due to the effect of roughness on the emissivity, however, brightness temperatures were actually 20°C warmer over the rough Sea. At high altitudes infrared equivalent black-body temperatures decrease because of atmospheric absorption.

In contrast, microwave brightness temperatures increase with altitude over both the smooth and rough parts of the Sea due to emission from the moist atmosphere. Over the smooth sea there is approximately a  $10^{\circ}\text{C}$  increase between the heights of 1,500 m (133°K) and 9,000 m (143°K). Over the rough sea, the increase is about  $9^{\circ}\text{C}$ , from about 153°K to about 162°K. Based on these measurements, the second term in Eq. (2) (for  $\theta = 0^{\circ}$ ) amounts to 16-17°K. This term represents the brightness temperature equivalent to the atmospheric emission. The transmissivity  $\tau$  in this case is about 0.90 to 0.95. Variations of  $T_b$  with nadir angle at higher altitudes are very similar to those at 1,500 m shown in Figure 2.

Figure 4 shows how measurements might be applied to sea state mapping from a spacecraft. Brightness temperatures are rendered as gray shades for each scan position which are displayed in a photographic image. The image is produced automatically by displaying the radiometer scans as lines on a TV screen. Low brightness temperatures correspond to dark shades. The pattern over the entire Salton Sea, as mapped by the scanning radiometer from a height of 11,000 meters, is readily apparent. The land surrounding the sea appears white because of its very high emissivities ( $\epsilon > 0.9$ ) with brightness temperatures generally higher than 260°K. The much darker shades over the sea correspond to a brightness temperature range of 140 to 165°K, depending on sea state. The areal extent of variations in the sea state are clearly evident with low brightness temperatures (dark shades) corresponding to smooth seas and high brightness temperatures signifying rough seas.

A similar map of brightness temperatures observed from 10,000 meters over the Pacific Ocean is shown in Figure 5. Again, the coastline can be clearly recognized, separating  $T_B > 260^\circ\text{K}$  over land from  $T_B < 150^\circ\text{K}$  over the water. As in Figure 4, the aircraft flew along the center of the image from bottom to top. The radiometer scanned perpendicularly across the image. Very smooth seas, with no apparent white caps were observed visually near the Coast. About 20 km from the Coast, the sea became rougher and white caps were sighted frequently (Figure 1). Unfortunately, in this case, we could not make the quantitative observations of surface windspeed that we made over the Salton Sea.

The lightest regions over the Ocean in Figure 5 represent brightness temperatures of about  $140^\circ\text{K}$ ; over the 20 km wide dark zone near the Coast, corresponding to the area where no white caps were observed we measured the lowest brightness temperatures of about  $133^\circ\text{K}$ . Near the bottom of Figure 5, where only few white caps were seen, we measured  $136^\circ\text{K}$ . The variation of brightness temperature with nadir angle is the same in this case as over the Salton Sea: There is a nearly constant temperature difference between rough and smooth sea at all nadir angles and brightness temperatures at  $\theta = 50^\circ$  are about  $20^\circ\text{C}$  lower than at nadir.

As yet, we are unable to explain the large brightness temperature difference between smooth sea and rough sea at the nadir; nor can we explain the larger than expected difference at all nadir angles. We speculate that this may be due to the effect of foam and spray which has not been included in the

theoretical calculations. This speculation seems to be substantiated by, as yet, unpublished surface based measurements (Edgerton, 1968) at 2.2 and 0.8 cm, and by aircraft measurements at 3.2 cm (Williams, 1968).

## CONCLUSIONS

We conclude that quantitative measurements of emitted microwave radiation from a sea surface can be interpreted in terms of surface roughness. The emitted radiation is apparently more sensitive to the formation of foam and/or spray on the sea surface than to the existence or orientation of larger scale wave slopes. Only the latter had been accounted for in theoretical computations so far. Measurements of emitted radiation may thus be directly related not only to the sea state but also to the magnitude of the surface winds, as the formation of foam and spray is intimately related to the prevailing winds. Our measurements show that this interpretation can be made at all nadir angles between  $0^\circ$  and  $50^\circ$ , even directly at nadir, which is in contrast to theoretical predictions. Scanning microwave radiometers at wavelengths longer than 3 cm, to minimize atmospheric interference (clouds), could be effective spacecraft sensors of sea state on a global scale.

The large brightness temperature variation with surface roughness at all nadir angles leads to the emphatic conclusion that it is not practical to measure sea surface temperatures in this wavelength range, as some have proposed. Water temperature differences of  $8^\circ\text{C}$ , as might typically exist across the Gulf

Stream, for example, will result in brightness temperature differences of less than  $2^{\circ}\text{C}$  which is much less than the variation of  $7^{\circ}\text{C}$  that we observed due to rather modest roughness variations over the Pacific Ocean (Figure 5).

## REFERENCES

- Buettner, J. K. 1963. "Regenortung von Wettersatelliten mit Hilfe von Centimeter-wellen," *Naturwissenschaften*, 50, pp. 591-592.
- Edgerton, A. 1968. "Passive Microwave Measurements of Snow, Ice, Soil and Water," Progress Report on Contract No. NOmr 4767(00) Aerojet General Corp., El Monte, Calif., 15 Aug. 1968.
- Nordberg, W., Conaway, Jack, and Thaddeus, P. "Measurements from Aircraft of Microwave Radiation Emitted by the Earth and Atmosphere," submitted to *Journal of Remote Sensing of Environment*.
- Oister, G. and Falco, C. V. 1967. Microwave Radiometer Design and Development, Final Report Contract No. NAS5-9680, pp. 63. Aerojet-General Corporation, Space Division, 9200 East Flair Drive, El Monte, California.
- Stogryn, A. 1967. "The Apparent Temperature of the Sea State at Microwave Frequencies," *IEEE Transactions on Antennas and Propagation*, AP-15, No. 2, pp. 278-286.
- Williams, G. F. 1968. "Microwave Radiometry of the Ocean," Presented at Manned Spacecraft Center, Houston, Tex., 18 Sept. 1968.

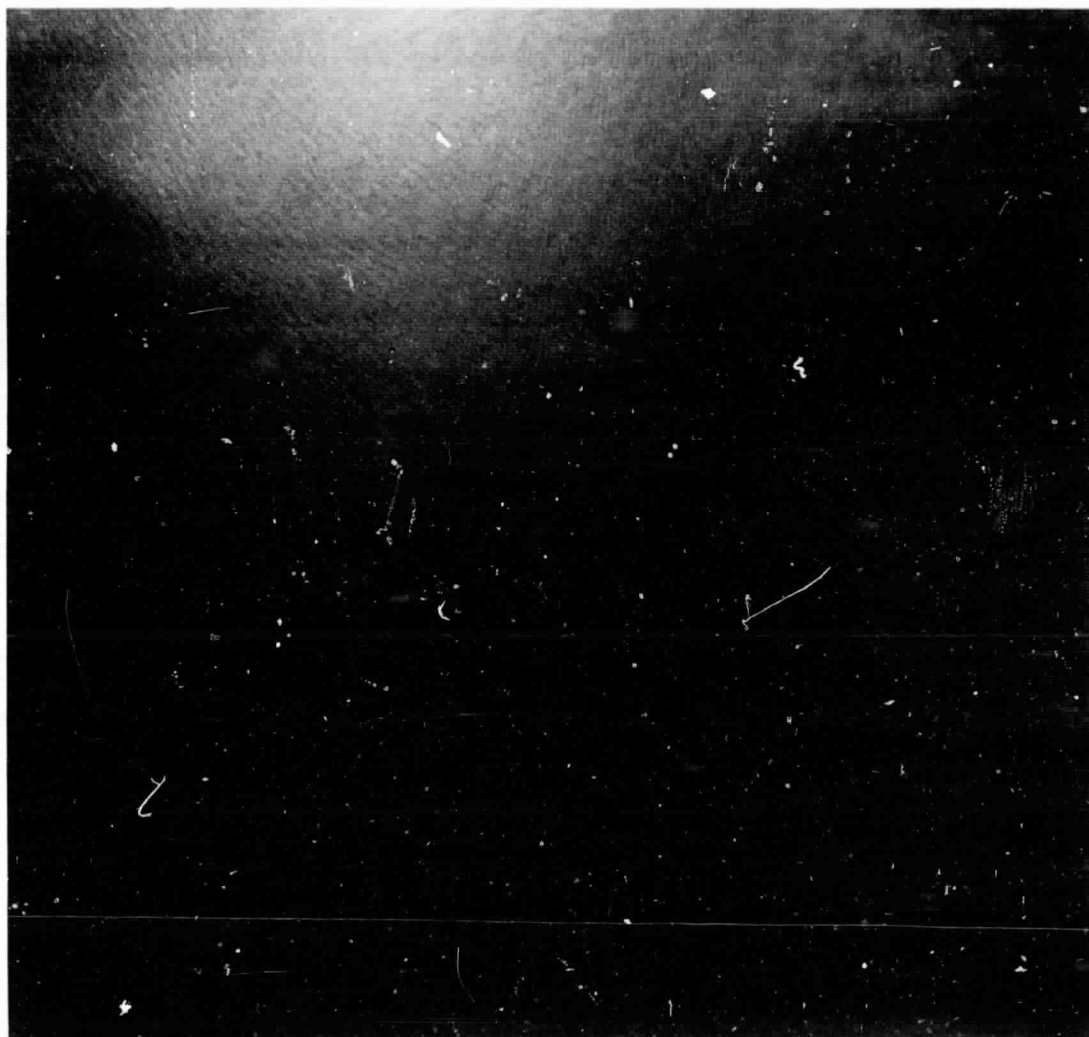


Figure 1

## FIGURES

Figure 1 - Print of a color photograph taken from a height of about 10,000 m over the Pacific Ocean, about 20 km off the coast of California. The change in sea surface roughness can be seen with rough water and white caps in the lower right and smooth water in the upper left. This corresponds to the area shown in Figure 5 where an increase in brightness temperatures can be noted. The aircraft path is from bottom to top along the center of this photograph.

Figure 2 - Observed and computed (Stogryn, 1967) brightness temperatures versus nadir angle at 1.55 cm over smooth and rough portions of the Salton Sea. Computations are for sea surface temperature of 290°K and a standard atmosphere. Observations were made with sea surface temperature of 294°K over the rough Sea and 300°K over the smooth Sea in a relatively moist atmosphere on 7 June, 1968. Each point shown for the observed data represents an average of six consecutive scans at the respective nadir angle.

Figure 3 - Brightness temperatures at 1.55 cm observed at nadir during four passes at varying heights along the center of the Salton Sea, California, on 7 June, 1968. Height (h) of aircraft is indicated at appropriate times. Equivalent black body temperatures ( $T_{IR}$ ) and reflectance of solar radiation ( $P$ ) measured by the MRIR radiometer are indicated over the appropriate time ranges.

Figure 4 - Pictorial image of brightness temperatures measured over Salton Sea, California, on 7 June 1968 from 11,100 meters. Dark shades correspond to low, light shades to high brightness temperatures. Times shown are GMT for indicated scans.

Figure 5 - Pictorial image of brightness temperatures measured off the coast of California near 40° North on 21 June, 1968. Dark shades correspond to low, light shades to high brightness temperatures. Times shown are GMT for indicated scans.

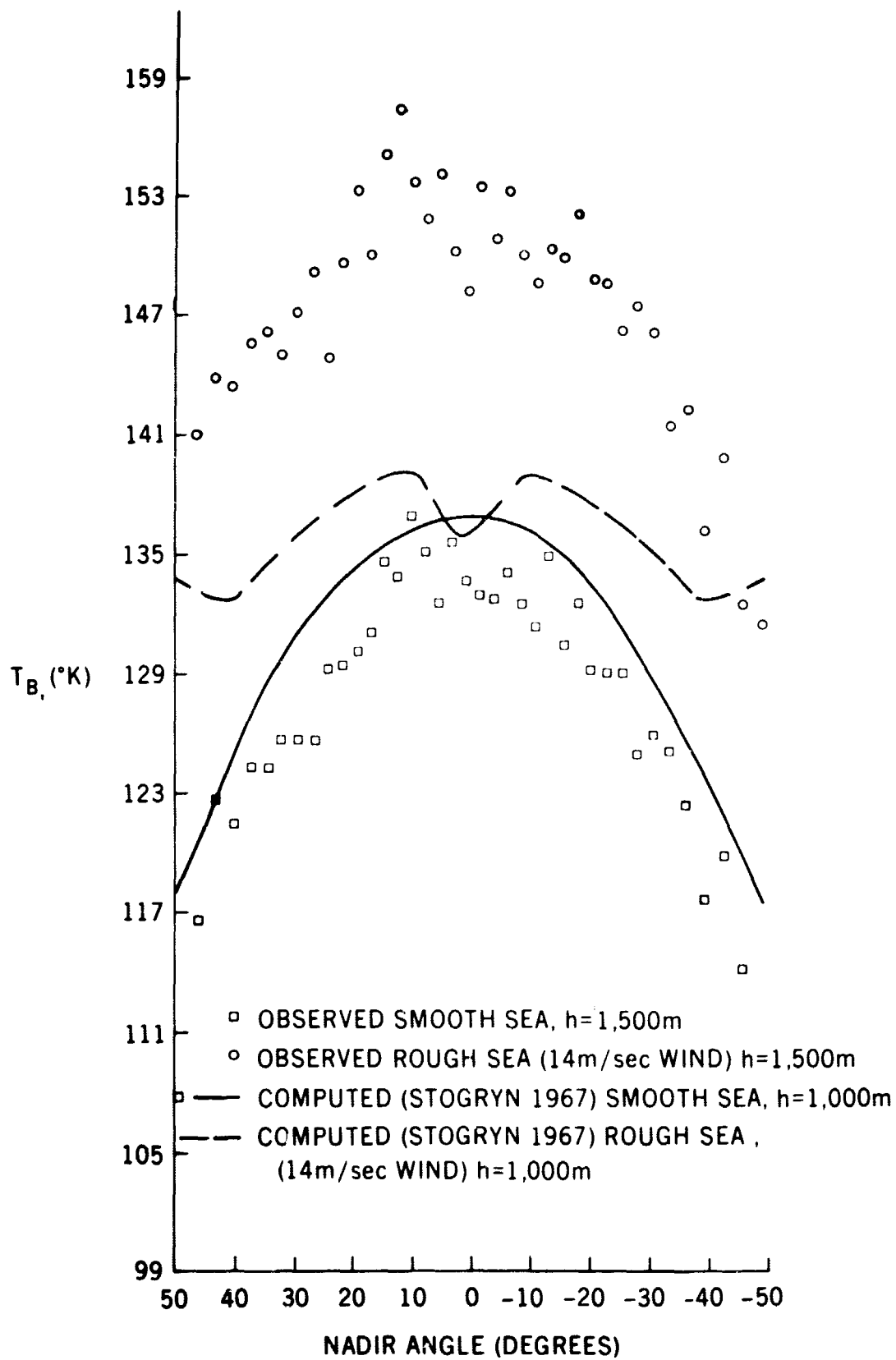


Figure 2

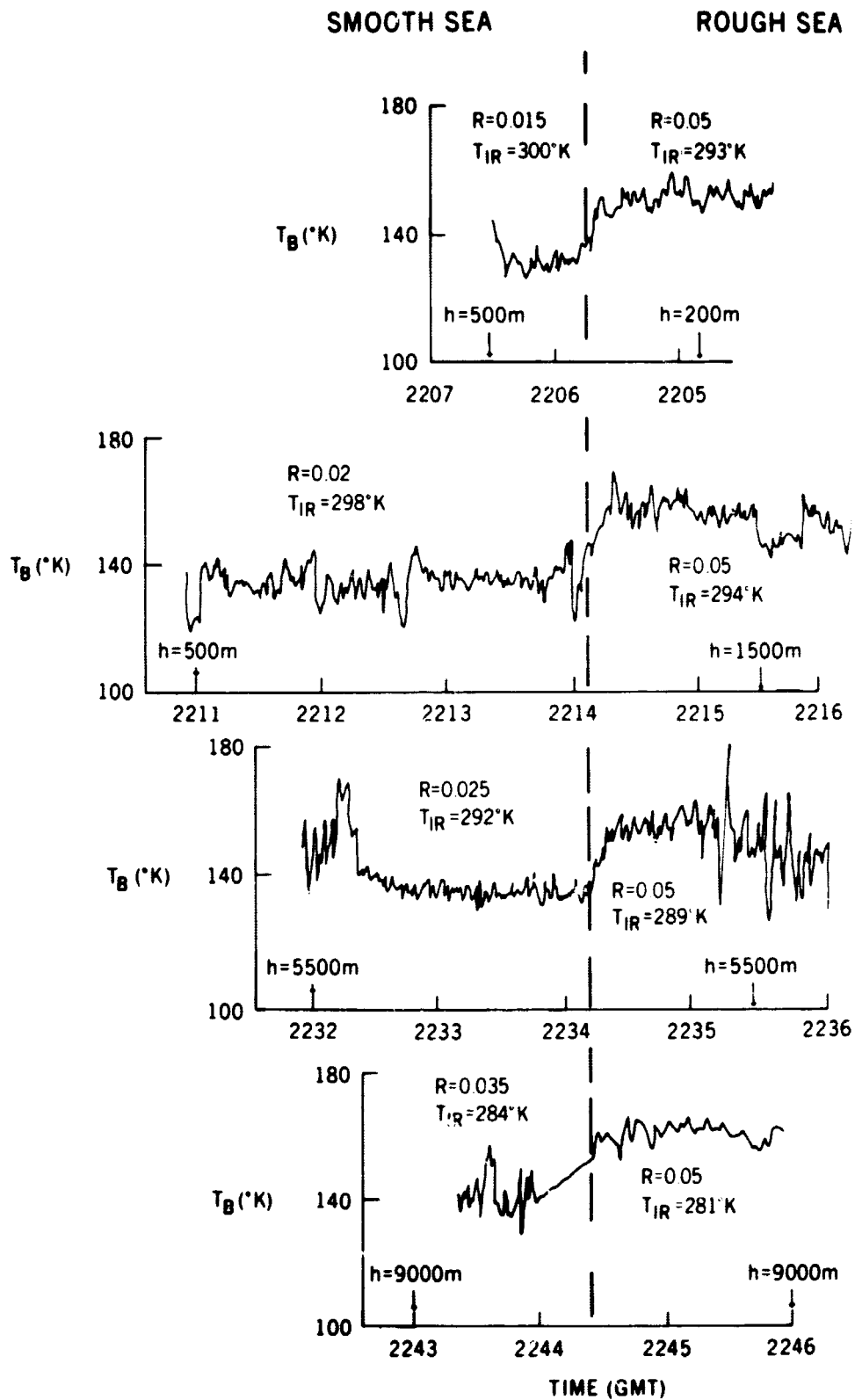


Figure 3

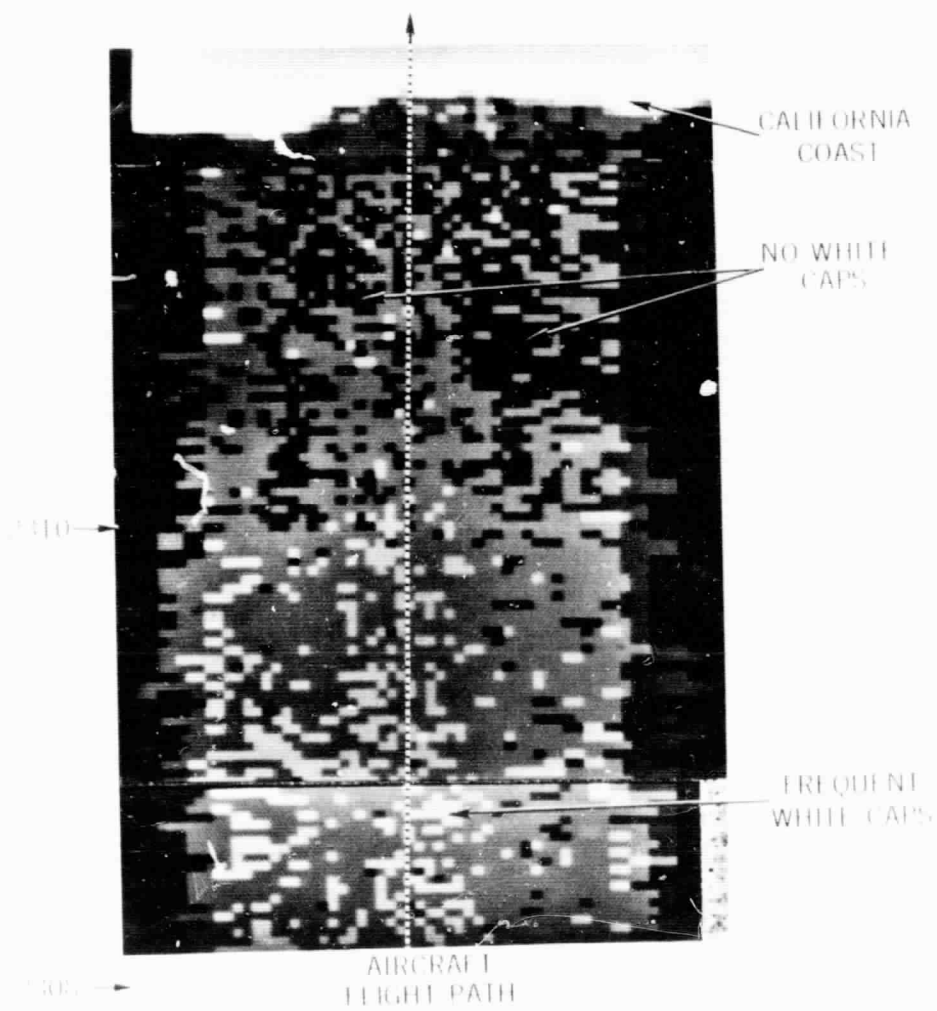


Figure 4

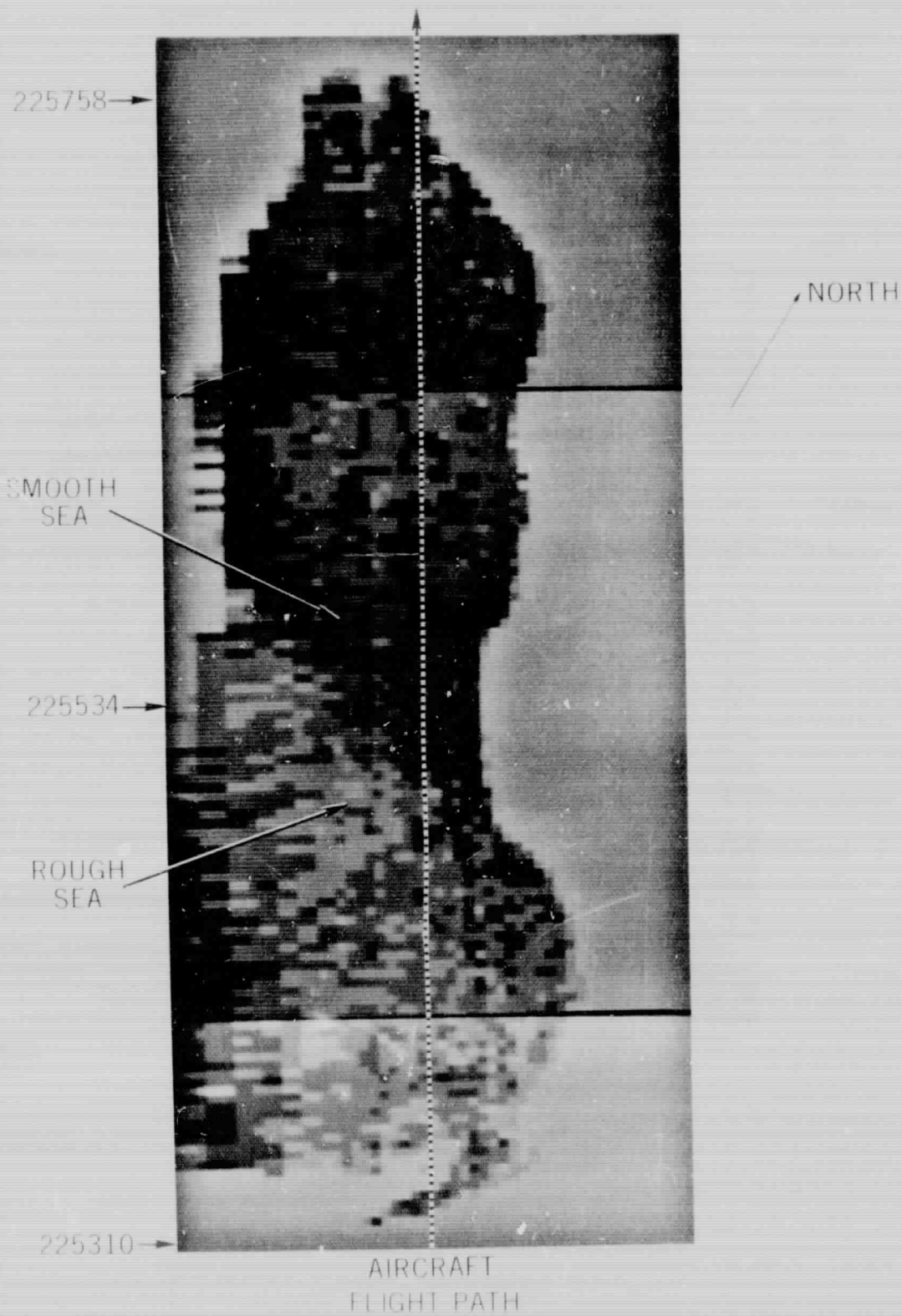


Figure 5